Invited paper

OPTO-ELECTRONICS REVIEW **11**(1), 7–17 (2003)

Free-standing non-polar gallium nitride substrates

H.P. MARUSKA*, D.W. HILL, M.C. CHOU, J.J. GALLAGHER, and B.H. CHAI

Crystal Photonics Inc, 5525 Benchmark Lane, Sanford, FL 32773

A review is given of efforts to prepare thick gallium nitride films on lattice-matched γ-$LiAlO_2$ substrates. Much progress in the design of new high performance nitride device structures is presently impeded by the lack of GaN substrates, leading to large defect concentrations in layers grown on foreign materials. These problems could be alleviated if a true GaN substrate were to become available, allowing homoepitaxial growth. The preparation of 50 mm diameter boules of γ-$LiAlO_2$ from the melt will be discussed, including wafer preparation. Growth of thick (300–400 μm) GaN layers on the γ-$LiAlO_2$ wafers will be presented. The GaN is deposited by the halide vapour phase epitaxy (HVPE) method. Characteristics of these 50 mm diameter wafers are explained in detail. Much progress has been made, but several problems remain to be overcome.

Keywords: nitrides, γ-$LiAlO_2$ wafers, GaN substrates, HVPE method

1. Introduction

Nitride-based semiconductor products have burst onto the scene in the last several years, and have now become a major player in the optoelectronics market. Revenues from the use of blue and green light-emitting diodes (LEDs) in the home and commercial lighting business alone are predicted to reach almost three billion dollars by 2009. Although the blue laser diode (LD) optical storage market is presently negligible, it is predicted to reach over the two billion dollar level by 2009. However, continued market growth is actually in doubt, because further increases in unit brightness levels for LEDs, which would allow penetration into the illumination industry, do not appear to be possible because the quality of present nitride materials is actually quite poor. It is still more difficult to coax even marginal performance levels and operating lifetimes out of the blue LDs, since their structures are filled with deleterious dislocations. Therefore, several organizations have taken certain new approaches, which they propose will solve the critical crystalline defect issues that limit the performance of gallium nitride (GaN) optoelectronic devices. Basically, they seek to prepare low defect density nitride substrates suitable for the homoepitaxial growth of near defect-free device material.

2. Substrate issues

We note that presently, most III-V nitride growth is accomplished in metal-organic vapour phase epitaxy (MOVPE) reactors, using trimethylgallium (TMG) and NH_3. These MOVPE reactors are generally used for growing the complex device structures found in LEDs and LDs which typically contain very narrow (quantum well) layers. GaN films have growth rates of 1–2 μm/hr in the MOVPE process; there is no practical way to grow free standing GaN wafers in such slow reactors.

The deposition of a low-temperature (500°C) buffer layer of AlN on sapphire substrates was the key discovery in 1988 by Akasaki for improving the surface morphology and crystalline quality of GaN epilayers [1]. The buffer layers serve to relax the strain between the GaN film and the sapphire. Although the buffer layer is highly dislocated, subsequent layers have far fewer dislocations. In spite of the buffer layers, GaN on sapphire routinely exhibit about 10^{10} dislocations/cm^2, although very specialized growth conditions have led on occasion to densities as low as 10^8.

2.1. Sapphire substrates

The development of a vapour phase growth process for preparing single crystal films of gallium nitride was originally commenced by Maruska on 13 May 1968 at the former RCA Laboratories (now David Sarnoff Research Centre) [2]. Maruska relied on the reaction between GaCl vapour and NH_3 in a hot-walled reactor, a halide vapor phase epitaxy (HVPE) system [3]. He used sapphire substrates simply because they were readily available due to a major on-going RCA program for silicon-on-sapphire growth. Sapphire offers a very large lattice mismatch with GaN, and these materials have very different thermal expansion coefficients. The thermal expansion problem creates tremendous compressional stresses during the cooling of GaN films. However, over the past thirty years, growth of GaN on sapphire, basically an accident, has become a tradition. This tradition always yields material that is severely compromised in crystalline quality, replete with dislocations and other lattice imperfections.

*e-mail: maruska@crystalphotonics.com

Despite many attempts at providing "buffer" layers such as amorphous AlN [4], the defects from the substrate mismatch propagate through the desired film. GaN films grown on sapphire are basically an ordered polycrystalline material. The individual crystallites are tilted with respect to one another, as well as twisted about the c-axis. As the understanding of the mechanisms of defect formation in the heteroepitaxial growth of III-V nitride thin films continues, the necessity for a homoepitaxial substrate has become very clear. While extended structural defects, such as dislocations, do not appear to be as active in quenching luminescent activity in nitrides when compared to phosphide or arsenide semiconductors, they certainly serve as optical scattering centres in coherent light emitters [5], as well as providing current leakage paths which limit operation at high bias levels [6]. In addition, current-crowding effects are known to be predominant in restricting power output levels for large area (> 300 × 300 μm^2), ultra-high brightness LEDs deposited on insulating substrates such as sapphire, because the devices' underlying conductive layers are generally quite thin [7]. It is also well known that large area LEDs operating at high current levels have reduced operating lifetimes due to the much larger densities of structural defects [8]. Finally, the (0001)GaN/(0001)Al_2O_3 system presents difficulties in laser facet cleavage since the six-fold symmetric cleavage directions in the GaN and sapphire (0001) plane normal to this growth surface are rotated 30° with respect to each other.

2.2. SiC substrates

SiC has a much closer lattice match to GaN than sapphire. While conducting SiC substrates can provide a vertical conduction path, lasers and LEDs grown on SiC substrates currently suffer from cracking problems related to tensile thermal stress in the nitride epilayer, as well as an interfacial conduction barrier, which increases the generation of heat in the device. SiC substrates are extremely expensive and size limited. The GaN/SiC heterojunction also features an interfacial potential barrier of ~0.5 V, which limits laser efficiency and device yields. In summary, extended structural defects are always found to exist in high densities (10^8–10^{10} cm^{-2}) in samples grown on SiC substrates [9]. Thus although presently popular, sapphire and silicon carbide substrates both impart very basic and probably insoluble problems to device fabrication attempts. Hence we need an alternative approach.

2.3. Substrates based on epitaxial lateral overgrowth (ELOG)

Epitaxially lateral overgrown GaN on sapphire has been developed to reduce the number of threading dislocations [10]. Basically, a thin (~2 μm) GaN film is first deposited on a sapphire substrate, followed by a 0.1 μm film of SiO_2. The SiO_2 is then patterned to form 2–3 μm wide stripe windows with a periodicity of about 10 μm. More GaN is now grown on the masked substrate. Material growing up through the windows continues to feature large densities of defects, but the GaN which grows out laterally across the SiO_2 tends to have less than 1×10^6 defects/cm^2. However, blue LEDs made with ELOG material have proven to be no better than ones made simultaneously with GaN grown directly on sapphire [11]. But all of the problems related to sapphire which were discussed above remain, so ELOG is no solution for LEDs.

ELOG wafers have indeed led to much improved blue laser diodes. For example, an InGaN-based laser has been described by Nakamura, grown on ELOG, with a ridge width of 3 μm and a length of 450 μm [12]. The threshold current density was 3 kA/cm^2, and with 490 mA applied at 8 volts bias, 420 mW of power was emitted at 408 nm [13]. But this was a "lucky laser," one which happened to be entirely fabricated over a masked region. Considering that there is always a void where the two overgrown wings meet, then there are only at most several 5 μm stripes, at certain intervals across the wafer, in which a good laser can be fabricated. In fact, a 3-μm ridge waveguide is probably the maximum width that a laser based on ELOG can manage. Thus ELOG lasers will always have yield problems, and their maximum power levels will be physically constrained.

2.4. GaN substrates

Real gallium nitride substrates would solve all of the problems. But no one has ever melted GaN. It has been determined that GaN still does not melt even at temperatures as high as 2300°C under a nitrogen pressure of 70 kbar! [14]. However, centimetre-sized GaN crystals have been formed in liquid gallium held under nitrogen pressures up to 20 kbar at temperatures approaching 1600°C at Unipress in Poland [15,16]. Dislocation densities in these crystals are as low as 10 cm^{-2}, and no GaN thin film on sapphire has ever matched this crystalline perfection [17]. InGaN/GaN blue LEDs emitting at 455 nm grown by MOVPE on Unipress substrates have proven to be twice as bright as devices grown simultaneously on sapphire substrates [18]. Nakamura grew a blue laser structure on a Unipress substrate which emitted 30 mW of power and had a lifetime of 3000 hours, far better than devices formed on conventional sapphire substrates [19]. Recent Unipress results confirm that their low dislocation density substrates lead to much improved laser performance [20]. Unfortunately, these extreme growth conditions are probably not practical commercially, and the samples remain small and irregular. If gallium nitride is ever to reach its full potential as an optoelectronic material, another method for growing large area single crystal wafers that can function as substrates for defect-free homoepitaxy will have to be found. Crystal Photonics Inc believes that the answer will be found by using new, perfectly lattice-matched $LiAlO_2$ wafers to supply substrates for the epitaxial growth of nearly defect-free

GaN. We are in the process of developing the optimised recipe for growing large (50 mm diameter) crystal boules of these oxides using the Czochralski method. We have demonstrated the growth of thick GaN films on wafers cut from these boules. The characteristics of these wafers will be discussed in this article.

3. Technical discussion: wafer growth processes

3.1. Choice of substrate

The unusual crystal structure of γ-$LiAlO_2$ was first elucidated by Marezio using flux-grown material, and he determined that the unit cell has four-fold (square) symmetry when looking down the *c*-axis [21]. The *c*-parameter of $LiAlO_2$ is 6.268 Å, while the a-parameter is 5.168 Å. Czochralski growth of γ-$LiAlO_2$ was first reported by Cockayne and Lent in 1981 [22]. Wafers were sawed from their boules and polished. They found that the material is transparent in the range of 200 to 4000 nm. They determined thermal expansion coefficients of $a_a = 7.1\times10^{-6}$ °C^{-1} and $a_c = 15\times10^{-6}$ °C^{-1}.

The possibility of growing GaN on γ-$LiAlO_2$ was first discussed by Hellman *et al*. in 1997 [23]. The a-c (100) plane of γ-$LiAlO_2$ has the same atomic arrangement as the (10$\underline{1}$0) prismatic face plane of the wurtzite structure. In fact, the *c*-parameter of γ-$LiAlO_2$ is close to 2 times $a_h = 6.378$ Å for GaN, while the a-parameter of $LiAlO_2$ is basically a perfect match to $c_h = 5.165$ Å for GaN. In 1998, Ke *et al*., using γ-$LiAlO_2$ grown by the temperature gradient technique, deposited GaN films about 350 nm thick by MOVPE on polished wafers at 1020°C [24]. Indeed, the GaN films featured the (10$\underline{1}$0) orientation, and the rocking curve on the (10$\underline{1}$0) peak had a FWHM of 530 arc-sec [25]. They noted that since the thermal expansion parameters of GaN are $a_a = 5.59\times10^{-6}$ °C^{-1} and $a_c = 3.17\times10^{-6}$ °C^{-1}, there will be considerable compressive stress in GaN films grown on γ-$LiAlO_2$ substrates. Recently, Waltereit *et al*. have grown (10$\underline{1}$0)-oriented GaN films by MBE on (100) γ-$LiAlO_2$ substrates [26]. They determined that the GaN films possess anisotropic in-plane stresses, with stress in the *a*-direction almost three times as large as in the *c*-direction, leading to anisotropy in dislocation structure [27]. They observed that AlGaN/GaN multiquantum well structures grown with this orientation exhibit a blue shift in cathodoluminescence wavelength compared with bulk GaN, while equivalent structures grown on (0001)-oriented GaN on sapphire are red-shifted below bulk emission wavelengths [28].

When grown on (100) oriented $LiAlO_2$, the GaN hexagonal cell will be oriented sideways, with the polar *c* axis in the plane of growth, which will have profound effects on polarization issues. Figure 1 provides a ball-and-stick model of the interface between $LiAlO_2$ and GaN. From this figure, it can be clearly seen why the GaN film has the (10$\underline{1}$0) orientation. We note that conventional growth of GaN on (0001) sapphire substrates gives material with a permanent electric dipole along the *c*-axis, leading to the quantum confined Stark effect in GaN quantum well structures [29]. This internal electric field leads to spatially indirect optical transitions for UV-emitting LEDs, creating much dimmer devices [30].

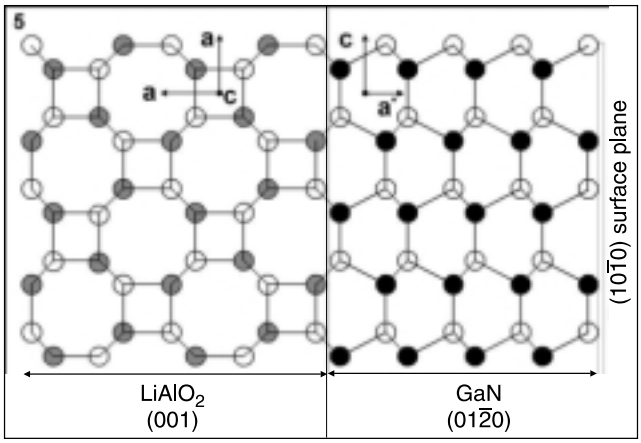

Fig. 1. The interface between $LiAlO_2$ and GaN, showing perfect matching.

3.2. Growth of $LiAlO_2$ crystal boules

$LiAlO_2$ melts at 1700 °C under atmospheric pressure. We have found that $LiAlO_2$ growth should be started by mixing an equimolar ratio of $LiCO_3$ and Al_2O_3. The mixture of the constituents are added to an iridium crucible which has a 100 mm diameter and is 112 mm high. This results in a stoichiometric composition. The loaded crucible is placed in a Czochralski crystal puller. After the crucible is placed in the furnace, heat is supplied inductively by a 50,000-W audio frequency generator. A $LiAlO_2$ seed crystal with *a*-axis (100) orientation is dipped into the melt while it is slowly rotating. Typically the crystal is pulled at a rate of 25 gm/hr. After 3 days of growth, boules are 50 mm in diameter and 200 mm long. Including sample preparation, heat-up, growth and cool-down, the crystal growth cycle takes 5 days. Boules are clear and transparent. An example is shown in Fig. 2.

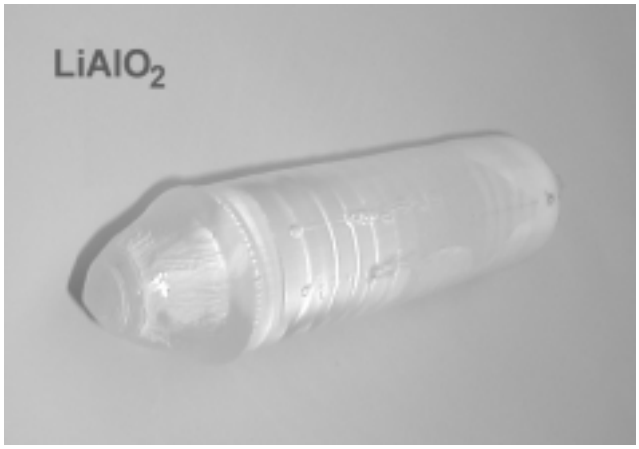

Fig. 2. Boule of γ-$LiAlO_2$ grown at Crystal Photonics.

3.3. $LiAlO_2$ wafer preparation

Wafers are sawed from the boule with a thickness of 500 μm, and polished to provide a smooth, clear surface. A wafer is shown in Fig. 3. The wafer surface is generally first prepared by chemo-mechanical polishing. Although such surfaces can appear to be completely smooth to the unaided eye, there are always scratches present, and at least several layers of surface atoms will be misplaced. Thus, prior to growth of a GaN film, the $LiAlO_2$ wafer is inserted in a 50% solution of hydrochloric acid for 20 minutes, followed by a rinse in distilled water and then methanol. The wafer is then spun dry.

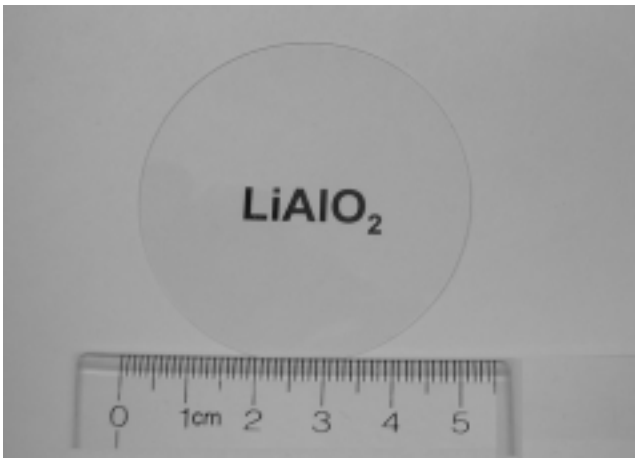

Fig. 3. Representative polished wafer of $LiAlO_2$.

3.4. HVPE growth of GaN

In recent years, a number of researchers have pursued halide vapour-phase epitaxy (HVPE) as a quasi-bulk technique for the growth of thick (> 20 μm), large-area GaN substrates [31–33]. Growth rates in the HVPE machines were very fast, ranging as high as 200 μm per hour (3–4 μm per minute) [34]. The thick layer growth is facilitated by the near-equilibrium nature of the process, which can be exploited to generate material with somewhat lower defect densities than other methods.

HVPE is based on using chlorides to transport the group-III species. HVPE is based on chemical equilibrium in a hot-walled reactor, where the typical reactions are

$$HCl + Ga \rightarrow GaCl + \frac{1}{2}H_2$$
$$GaCl + NH_3 \leftrightarrow GaN + HCl + H_2$$

GaCl can be delivered to the substrate at much higher flow rates than trimethylgallium without incurring gas phase nucleation problems, and the efficiency of ammonia use is greatly improved due to the effects of Cl on the N-H bonds. Thus, growth rates exceeding 50 μm/hr are readily obtained.

Following established practices, Crystal Photonics has designed and constructed an HVPE reactor for the rapid growth of GaN films. This reactor is shown in Fig. 4. All GaN wafers have been grown in this reactor.

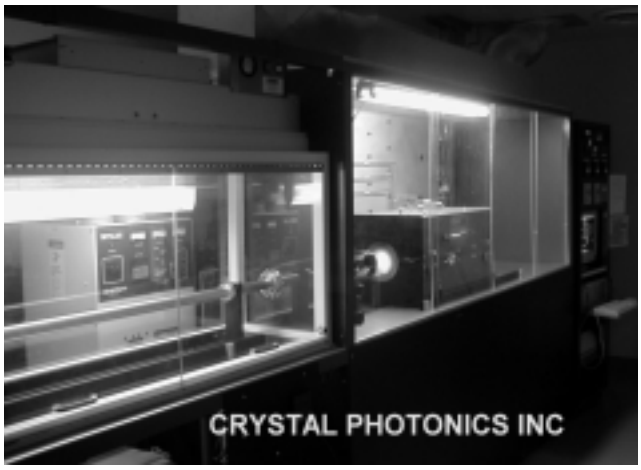

Fig. 4. Crystal Photonics HVPE reactor for preparing GaN wafers.

The growth chamber is horizontal and contains 3 temperature zones. Both zone one and zone three are each nine inches long, while the middle zone two is six inches long. The wafer rests in a chuck on a rotating spindle located at the boundary between zone one and zone two. The quartz boat filled with metallic gallium is placed in zone three.

The prepared $LiAlO_2$ wafer is mounted on a SiC-coated graphite chuck and placed in the load lock of the HVPE reactor. The chuck is carried on an alumina insertion rod. The three furnace zones are typically set at 875–875–850°C. Nitrogen is set to flow through all gas lines, except for the GaCl generation tube, in which hydrogen flows. Hydrogen prevents possible oxidation of the Ga surface and provides control of the growth rate. After the load lock is opened, the sample is moved to a pre-heat zone and slowly brought up to growth temperature. Then the chuck is inserted into the furnace, and placed in a dish located on the rotating spindle. The insertion rod is withdrawn, and the chuck is spun at 60 rpm. Flow of ammonia at a rate of 1 sLm commences. After 7 minutes of baking in ammonia, the flow of HCl is started, and one minute later, deposition of GaN commences on the substrate. Typically, the HCl flowrate is 20 sccm. A run usually proceeds for 6 hours. The chuck is then recovered by the insertion rod, transferred into the preheat zone, and cooled slowly to room temperature. Unless the wafer is cooled slowly, it will fracture. The growth rate is set to be about 50 microns per hour. Thus, our GaN wafers are always at least 300 microns thick. Many analytical procedures have been undertaken in order to understand the characteristics of these wafers.

3.5. GaN wafer preparation

As noted above, there are significant differences in thermal expansion between GaN and $LiAlO_2$, and wafer bowing must be prevented. Slow cooling has proven to be very helpful in this respect. Fortunately, $LiAlO_2$ is relatively soft, and tends to cleave apart into many pieces upon cooling. These pieces simply fall away from the GaN wafer. Remaining $LiAlO_2$ material can be etched away in hydrochloric acid. A typical GaN wafer is shown in Fig. 5. After the $LiAlO_2$ has been removed, the rear surface of the GaN (the surface which was in contact with the $LiAlO_2$) is always smooth and shiny. However, the front surface is not smooth. The front surface is always covered with certain morphological features which we term "arrowheads." These "arrowheads" can be seen in Fig. 6, and will be discussed further below.

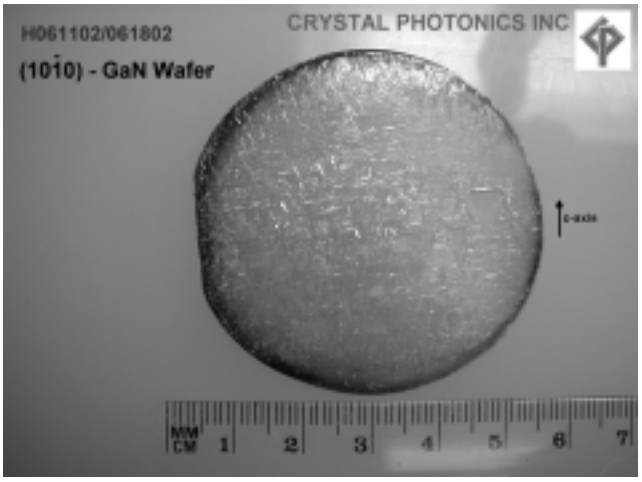

Fig. 5. Free-standing 50 mm diameter GaN wafer.

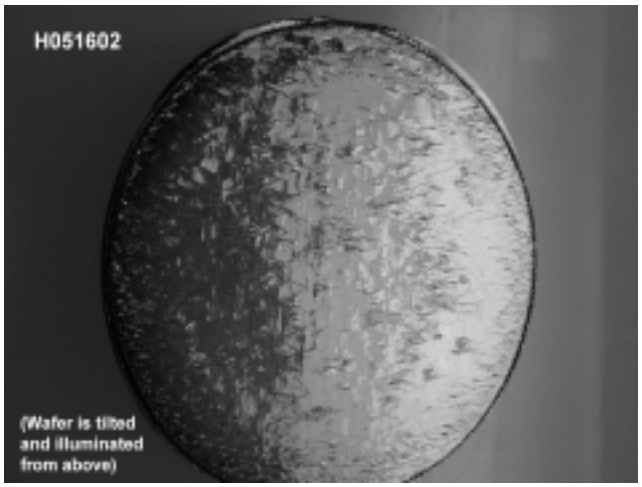

Fig. 6. View of the "arrowhead" features on the wafer surface.

4. Technical discussion: wafer characterization

4.1. X-ray analysis

All X-ray studies were performed at Rigaku Laboratories in Houston. Coupled $\theta/2\theta$ image collection and theta high resolution rocking curves were obtained with the high resolution ATX-G Thin-Film Diffractometer and D/MAX--Rapid Micro-diffractometer. γ-$LiAlO_2$ wafers have been studied with a two-dimensional detector scan. The 2D detector data, which observes a large section of the Debye ring, shows in all cases that every reflection is accounted for by the γ-$LiAlO_2$ phase. The $\theta/2\theta$ scan shows that the *a*-axis is normal to the surface (only the <200> reflection is observed). The rocking curves on the (200) peak are symmetrical and well defined, with a representative FWHM of 169 arcsec, indicating perfect single crystals.

Representative results for GaN wafers are shown in Fig. 7 and Fig. 8. In all cases, the wafers were found to have the (10$\underline{1}$0) orientation, which places both the *a*- and the *c*-axes in the plane of the sample. The rocking curve shown in Fig. 8 has a FWHM of 576 arc-sec, which is comparable to the typical results on sapphire substrates with MOVPE growth [35].

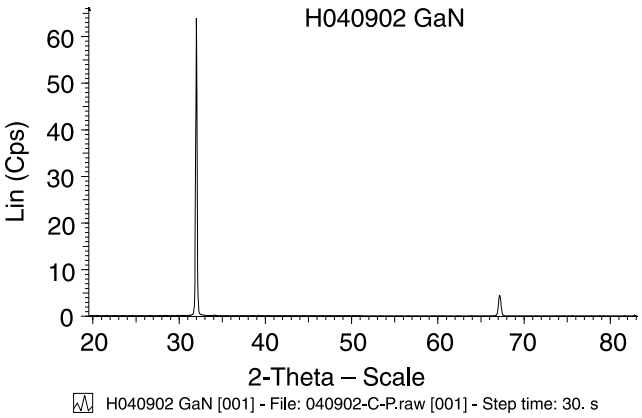

Fig. 7. $\theta/2\theta$ scan of free standing GaN wafer, indicating (10$\underline{1}$0) orientation.

4.2. Surface studies

The surface morphology of the GaN wafers has been studied by using conventional optical microscopy and a JEOL 840 scanning electron microscope. $LiAlO_2$ is much softer than GaN, and is much more easily fractured. Figure 9 shows an optical photomicrograph of a $LiAlO_2$ wafer on which was grown a relatively thin (10 micron) film of GaN. When the wafer was removed from the reactor, the GaN film broke away from the substrate. But notice, there is still a portion of $LiAlO_2$ attached to the bent GaN film. The fracture actually occurred within the $LiAlO_2$. It is clear that the differences in the rate of thermal contraction create tremendous strains within these adjacent materials, and basically all GaN films on $LiAlO_2$ undergo fracture at thick-

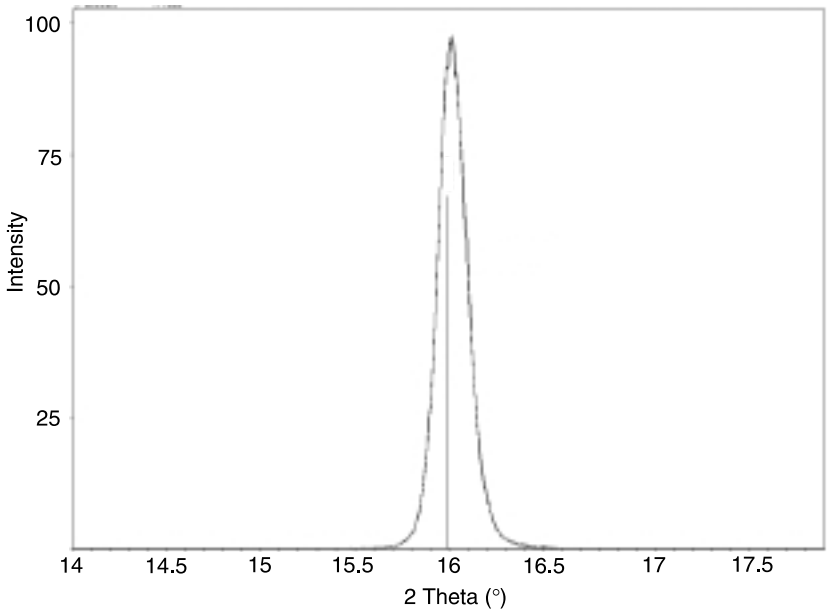

Fig. 8. Rocking curve for (10$\bar{1}$0) peak of GaN wafer.

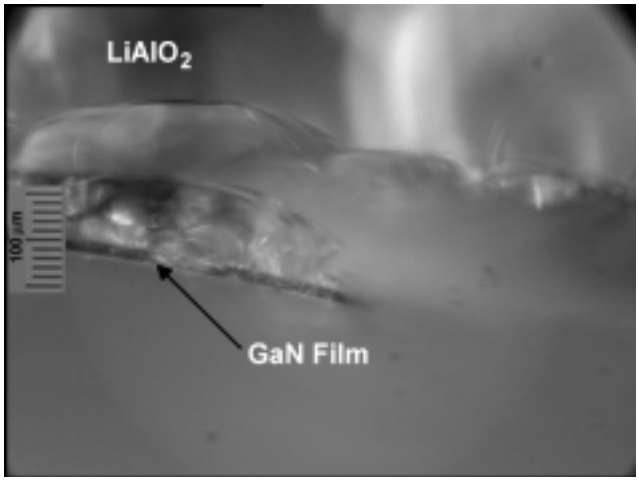

Fig. 9. A thin film of GaN will fracture the surface of $LiAlO_2$ upon cooling.

nesses below about 50 microns. But for GaN films of thicknesses of several hundred microns, only the $LiAlO_2$ has been observed to fracture.

Figure 10 shows an SEM image of a 4.5 mm wide region of the surface of a free standing GaN wafer. This area of the surface is quite smooth, and it appears shiny when observed visually. Figure 11 shows the surface of another wafer under higher magnification. Again, most of the region is quite smooth, although a dark defect which is the form of a line is apparent. Figure 12 shows a cross-sectional image of a wafer. Once again, the smoothness of the surface is quite apparent. The original $LiAlO_2$ substrate was on the left side of the image.

In addition to smooth surface areas, we have also observed discreet defects which are basically triangular in shape, which we call "arrowheads." X-ray analysis has

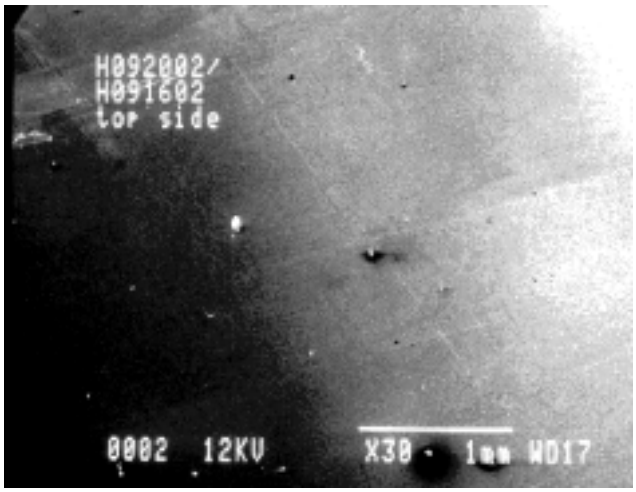

Fig. 10. Representative smooth surface area of a free-standing GaN wafer.

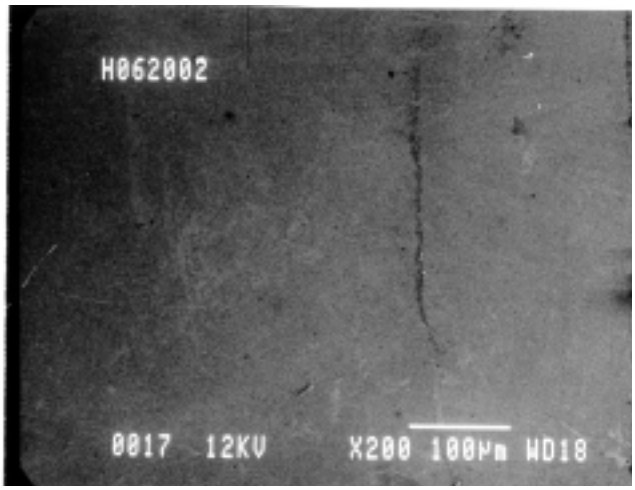

Fig. 11. View of the surface of another GaN wafer, showing a line of defects.

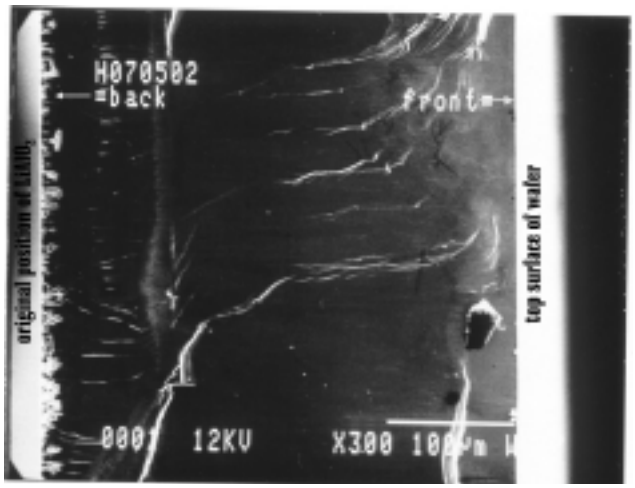

Fig. 12. Cross section of a typical GaN wafer.

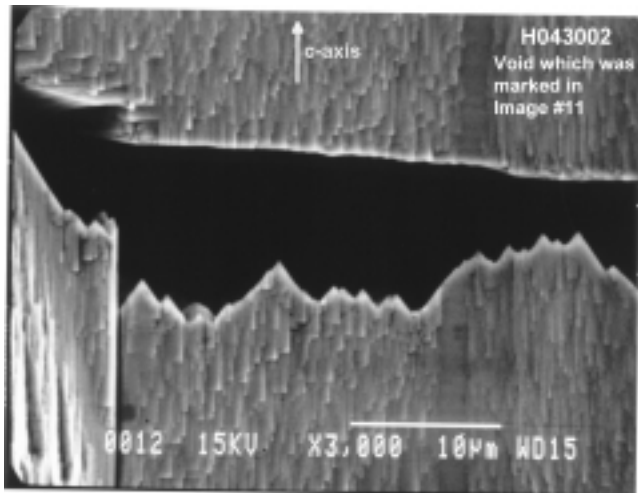

Fig. 14. Details of a surface void incorporated in an arrowhead.

shown that the *c*-axis always runs along the spine of these arrowheads, as noted in Fig. 13. Thus the base of an arrowhead is the (0001) plane. Surrounding surface regions are flat. The arrowhead shown in Fig. 13 contains a small void, which is depicted at higher magnification in Fig. 14. All such voids which have been found on many wafers always have the same asymmetrical shape. One surface has a corrugated appearance, while the opposite surface is relatively smooth, in some instances completely flat. It can be expected that one of these (0001) surfaces may have Ga polarity, while the opposite face may have N-polarity. Figure 15 shows a void in cross-sectional view of a wafer. In this image, we are looking down the *c*-axis, at the (0001) plane. Notice the hexagonal columns. They are all mutually aligned. Similar *c*-axis oriented hillocks have been observed in GaN crystals grown by the reaction between gallium and ammonia [36]. The hillock formation, which was observed when the crystals were viewed along the *c*-axis, was attributed to a breakdown of the interface due to rapid growth. The void which is shown in Fig. 15 is located approximately in the center of the wafer, halfway from either the upper or the lower surface. Notice that the void closed over as growth continued, and we believe that our growth rate is constant during the entire run. The void shown in Fig. 14 is on the upper surface of the wafer, and it probably would also have grown over if growth had continued for that sample. In our case, since growth is aligned in the (10$\underline{1}$0)-direction, the hillocks are actually rotated 90° away from the growth direction. The origin of these voids is under further investigation.

The rear surface of a typical GaN wafer is shown in Fig. 16. First of all, this surface was originally in contact with a smooth, polished surface of $LiAlO_2$, so this rear surface always appears to be very shiny to the unaided eye. However, defects become visible at high magnification, as seen in Fig. 16. There are large numbers of circular or oval defects, plus what appear to be cracks. It is likely that these cracks are a result of the more rapid thermal contraction of $LiAlO_2$, which stresses the GaN rear surface. The $LiAlO_2$ wafer fractures into stripes which are aligned with the

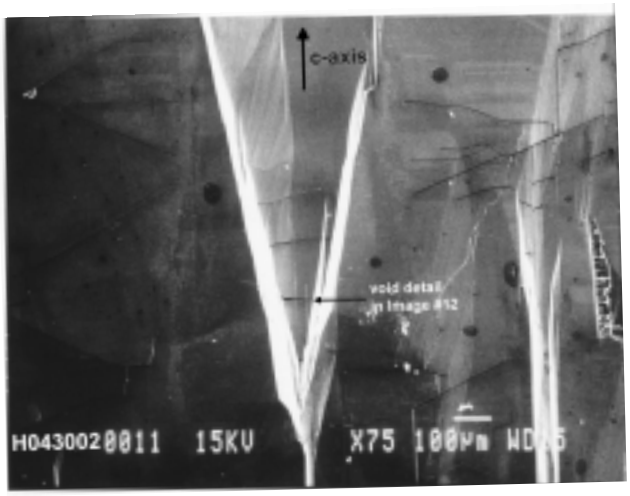

Fig. 13. Raised triangular defect on wafer surface which we call an "arrowhead."

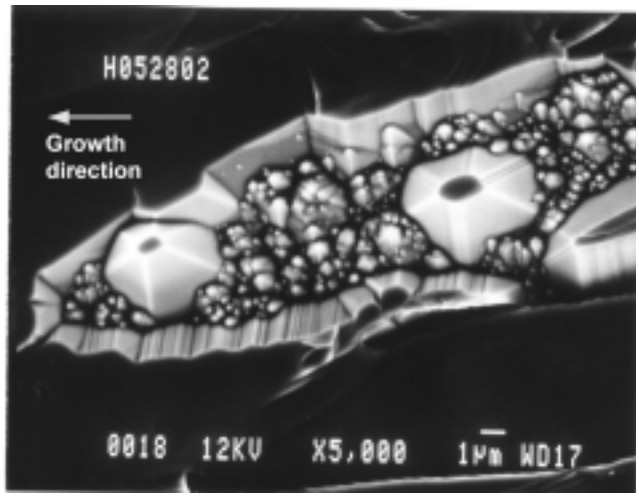

Fig. 15. Details of a void, observed in cross-section.

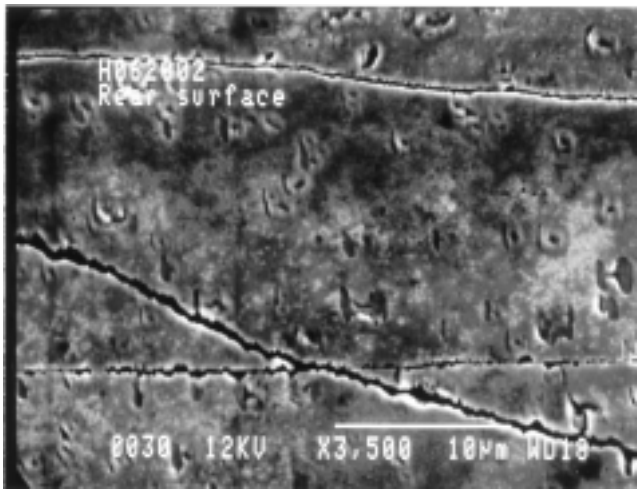

Fig. 16. View of the rear surface of a GaN wafer, showing cracks and round defects.

cracks in the GaN wafer. The GaN cracks run about 10 microns deep.

4.3. Elemental analysis

There is much concern about incorporation of Li and Al into the GaN wafer. After all, the $LiAlO_2$ wafer is constantly exposed to an environment containing HCl. Although the front surface of the wafer is rapidly covered by GaN, the rear surface is seated on the chuck, and it is possible for HCl vapours to diffuse between the chuck and the wafer. If LiCl or AlCl vapours are formed, these species will be volatile at the growth temperature.

The elemental constituency of the rear surfaces of the GaN wafers has been probed by energy dispersive x-ray spectrometry (EDS) in the SEM. The wafers were first thoroughly etched in HCl to remove all traces of $LiAlO_2$. EDS always indicated the presence of Al and O, as well as Ga and N, on the rear surface. EDS is not sensitive to Li. Front surfaces of wafers showed only the spectra for N and Ga.

A wafer was subjected to secondary ion mass spectrometry (SIMS). In a SIMS analysis, an ion beam (oxygen in our case) is used to bore a hole in the sample, and the masses of the ejected particles are analysed. We calibrated the SIMS instrument by first preparing GaN samples which had been implanted with known doses of Li. The instrument already had an Al calibration. The results are shown in Fig. 17. Heavy concentrations of both Li and Al were found to be incorporated in the first 3 microns of material from the rear surface. There was also evidence for chlorine, but this may have come during the etching procedure to remove the substrate. Li was still above the background level for the instrument (10^{15} atoms/cm^2) at a depth of 12 microns. Al was at the background level after about 4 µm.

Figure 18 shows a SIMS depth profile from the front of a GaN wafer. Notice that the depth scale is much smaller than the one for the back surface. Although there was seen a Li and an Al signal down to 0.3 microns, these are considered to be surface contamination problems. At further depths, both signals are at the instrument limits. Therefore, although there is abundant incorporation of both Li and Al in the rear surface of the wafer, there is no evidence of these species in the top surface. Therefore, vapour transport of Li or Al is not a problem in our reactor, and the presence

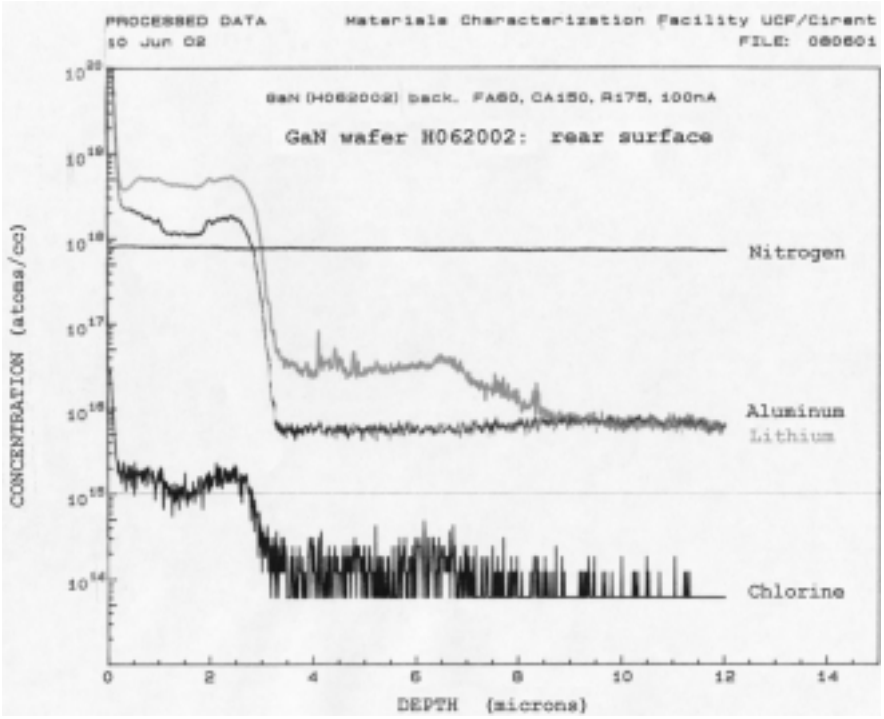

Fig. 17. SIMS depth profile for the rear surface of a GaN wafer.

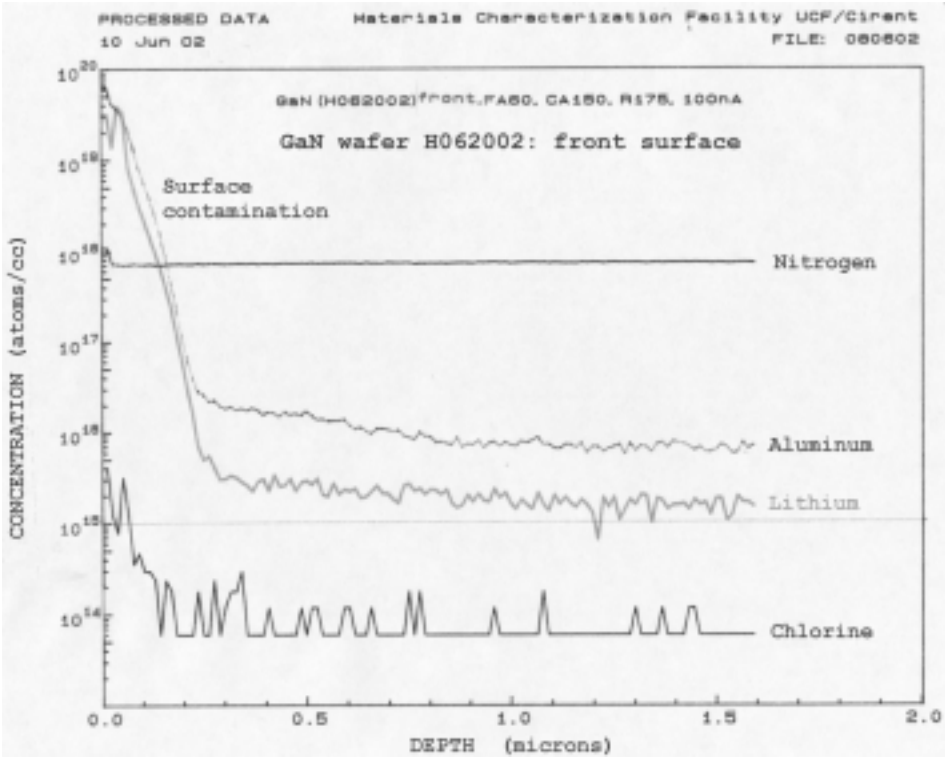

Fig. 18. SIMS depth profile from the front surface of a GaN wafer.

of these impurities in the rear surface must be the result of diffusion.

The front and rear surfaces of a wafer were studied using SIMS elemental analysis imaging. The results are shown in Figs. 19 and 20. The images were obtained by scanning the ion beam over the central region of the wafer while collecting the SIMS data. The center of each image is dark due to a problem with the instrumental detector system. Figure 19 shows strong signals for Ga, Al and Li over the entire rear surface of the wafer. Ga of course serves as a standardization factor. This result is consistent with the depth profile of Fig. 17.

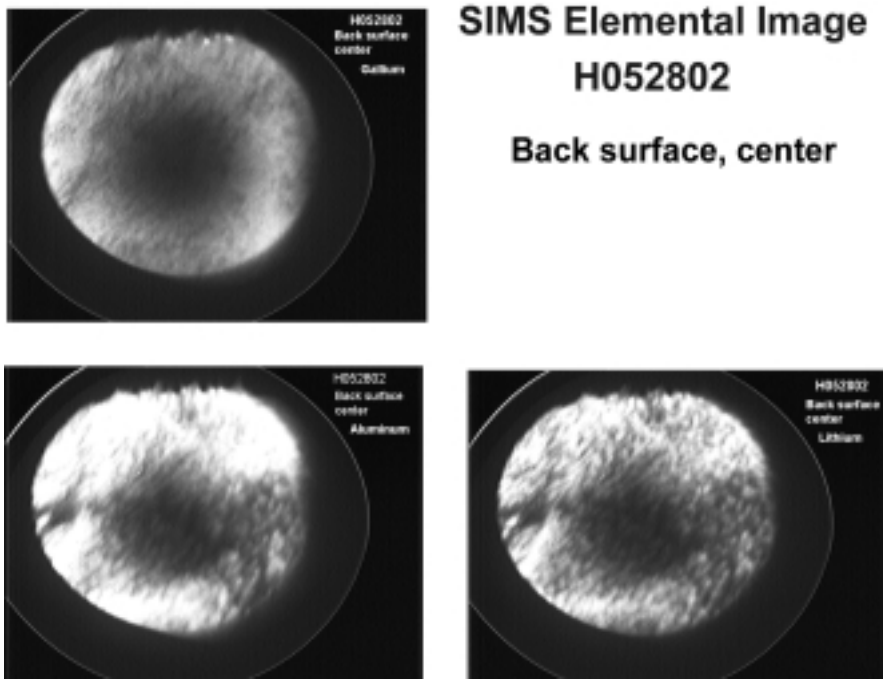

Fig. 19. SIMS elemental image analysis of the rear surface of GaN wafer.

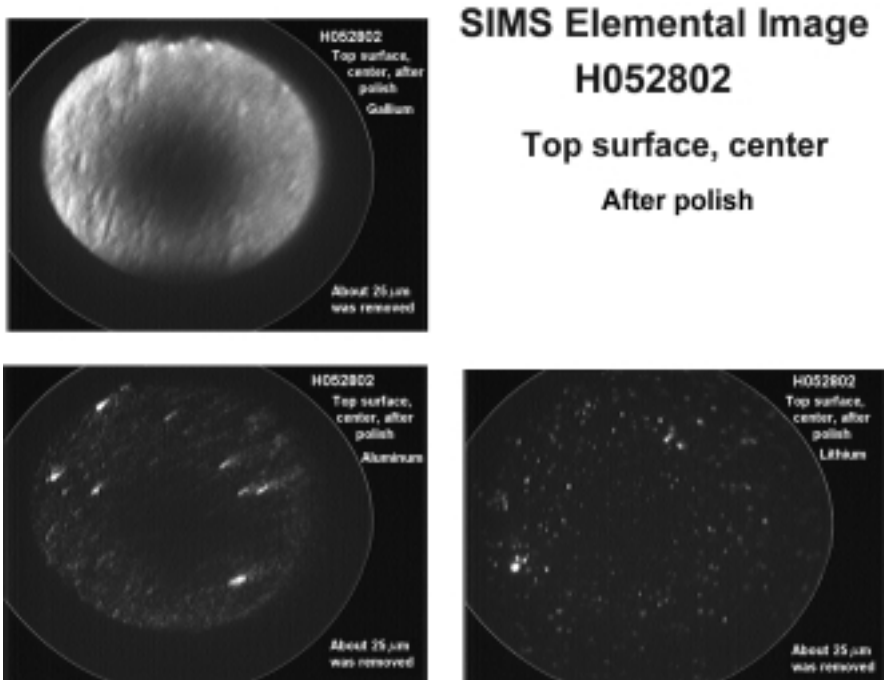

Fig. 20. SIMS elemental image analysis of front surface of GaN wafer.

Figure 20 shows the SIMS elemental images for Ga, Al and Li determined at the front of the wafer. Although the Ga image is quite clear and uniform as expected, there are no Li or Al signals (the small bright spots are due to noise). Again, this result shows that Li contamination of the wafer is not an issue.

A number of Hall effect samples were prepared from the GaN wafers [37]. All wafers were n-type with carrier concentrations in the low to mid-10^{18} cm^{-3} range. The best result was obtained for a wafer which was 205 microns thick. It was found that n = 6.5×10^{18} cm^{-3}, with a mobility of 174 cm^2/Vs. Such results are quite typical for GaN films grown by HVPE. But these values are far superior to earlier results for GaN films grown on $LiGaO_2$ by MOVPE, which were heavily contaminated with Li, and had carrier concentrations exceeding 1×10^{20} cm^{-3} with mobilities around 10 cm^2/Vs [38].

5. Conclusions

A program has been launched which seeks to produce high quality free standing 50 mm diameter gallium nitride substrates. Preliminary results have been reviewed. First of all, a method has been developed for pulling large crystalline boules of γ-$LiAlO_2$ from the melt. Crystals are 50 mm diameter and 200 mm long. X-ray studies indicate that the material is single phase with excellent crystallinity.

A new HVPE reactor has been constructed and it is used for growing thick films of GaN onto γ-$LiAlO_2$ wafers, after these substrates have been polished and etched. Growth rates are typically 50 μm/h. GaN wafers are in general 300–350 μm thick. These wafers readily delaminate from the γ-$LiAlO_2$ substrate, which tends to fracture into a large number of chips. Residual $LiAlO_2$ is removed by etching. The resulting 50 mm diameter GaN wafers have been characterised by several procedures.

X-ray diffraction studies have shown that all GaN wafers have the (10$\underline{1}$0) orientation. Thus the polar *c*-axis resides in the wafer plane. The best wafer exhibited a FWHM for the (10$\underline{1}$0) rocking curve of 576 arc sec. Major areas of the surfaces of wafers are quite smooth. Surface roughness is on the order of 0.5 μm. However, surfaces always contain discreet triangular defects which resemble "arrowheads." These arrowheads always point in the direction of the *c*-axis. Micron sized voids have been observed on the surface of these arrowheads. The voids are always much longer than they are wide, and the short dimension is always oriented along the *c*-axis as well. One side of each void contains hillocks, while the other side is smooth. These features may indicate the Ga-surface and the N-surface. At present, transmission electron microscopy studies are underway to help define the nature of these defects.

Impurity incorporation has been studied by SIMS analysis. The rear surface of the GaN wafer contains high concentrations of Li and Al to a depth of 2–3 μm. Concentrations fall to the background level at about 12 μm deep. Neither Li nor Al was found to exist at levels above background on the front surface. This is consistent with electrical property measurements, which reveal donor concentrations in the low to mid-10^{18} cm^{-3} range, with electron mobilities approaching 200 cm^2/V-s.

Great efforts are being undertaken to provide an understanding of crystalline defects in these wafers. A clear understanding will allow us to make necessary improvements in the processing schedule so that we soon expect to pro-

vide GaN wafers that yield optoelectronic devices which far exceed the qualities of devices which are presently grown on sapphire.

Acknowledgement

The work was partially supported by DARPA contract number F19628-02-C-0057, monitored by Dr. J. Lorenzo and Dr. J. Carrano.

References

1. I. Akasaki and H. Amano, *Appl. Phys. Lett.* **56**, 185 (1988).
2. H.P. Maruska and J.J. Tietjen, *Appl. Phys. Lett.* **15**, 327 (1969).
3. H.P. Maruska, L.J. Anderson, and D.A. Stevenson, *J. Electrochem. Soc.* **121**, 1202 (1974).
4. K. Hiramatsu, *J. Crystal Growth* **115**, 628 (1991).
5. Z.L. Liau, R.L. Aggarwal, P.A. Maki, R.J. Molnar, J.N. Walpole, R.C. Williamson and I. Melngailis, *Appl. Phys. Lett.* **69**, 1665 (1996).
6. M.A. Khan, M.S. Shur, J.N. Kuznia, Q. Chen, J. Burm, and W. Schaff, *Appl. Phys. Lett.* **66**, 1083 (1995).
7. H. Kim, S.J Park, and H. Hwang, *IEEE Trans. Electron Dev.* **48**, 1065 (2001).
8. M. Hansen, P. Kozodoy, S. Keller, U. Mishra, J. Speck, and S. DenBaars, *Proc. 2nd Int. Symp. Blue Laser and Light--Emitting Diodes*, Chiba, Japan, 29 Sept. – 2 Oct., 1998.
9. S.D. Lester, F.A. Ponce, M.A. Craford, and D.A. Steigerald, *Appl. Phys. Lett.* **66**, 1249 (1995).
10. A. Sakai, H. Sunakawa, and A. Usui, *Appl. Phys. Lett.* **71**, 2259 (1997).
11. S. Nakamura, in *Introduction to Nitride Semiconductor Blue Lasers and Light Emitting Diodes,* edited by S. Nakamura and S.F. Chichibu, Taylor & Francis, 2000.
12. T. Mukai, K Takekawa, and S. Nakamura, *Jpn. J. Appl. Phys.* **37,** L839 (1998).
13. S. Nakamura, "Development and future prospects of InGaN-based LEDs and LDs", in *Introduction to Nitride Semiconductor Blue Lasers and Light Emitting Diodes*, edited by S. Nakamura and S.F. Chichibu, Taylor & Francis, 2000.
14. J. Karpinski and S. Porowski, *J. Cryst. Growth* **66**, 11 (1984).
15. M. Lesczynski, I. Grzegory, and M. Bockowski, *J. Cryst. Growth* **126**, 601 (1993).
16. S. Porowski, M. Bockowski, B. Lucznik, M. Wroblewski, S. Krukowski, I. Grzegory, M. Leszczynski, G. Nowak, K. Pakula, and J. Baranowski, *Mater. Res. Soc. Symp. Proc.* **449**, 35 (1997).
17. S. Porowski, *MRS Internat. J. Nitride Semic. Res.* **4S1**, G1.3 (1999).
18. M. Kamp, C. Kirchner, V. Schwegler, A. Pelzmann, K.J. Ebeling, M. Leszczynski, I. Grzegory, T. Suski, and S. Porowski, *MRS Internet J. Nitride Semic. Res.* **4S1**, G10.2 (1999).
19. I. Grzegory, *Acta Physica Polonica* **A98**, 2985 (2000).
20. V.Yu. Ivanov, M. Godlewski, H. Teisseyre, P. Perlin, R. Czernecki, P. Prystawko, M. Leszczynski, I. Grzegory, T. Suski, and S. Porowski, *Appl. Phys. Lett.* **81**, 3735 (2002).
21. M. Marezio, *Acta Cryst.* **19**, 396 (1965).
22. B. Cockayne and B. Lent, *J. Crystal Growth* **54**, 546 (1981)
23. E.S. Hellman, Z. Liliental-Weber, and D.N.E. Buchanan, *MRS Internet J. Nitride Semic. Res.* **2**, 30 (1997).
24. X. Ke, X. Jun, D. Peizhen, Z. Yongzong, Z. Guoqing, Q. Rongsheng, and F. Zujie, *J. Crystal Growth* **193**, 127 (1998).
25. K. Xu, J. Xu, P. Deng, R. Qiu, and Z. Fang, *Phys. Stat. Solidi* **A176**, 589 (1999).
26. P. Waltereit, O. Brandt, M. Ramsteiner, A. Trampert, H T. Grahn, J. Menniger, M. Reiche, R. Uecker, P. Reiche, and K.H. Ploog, *Phys. Stat. Sol.* **A180**, 133 (2000).
27. P. Waltereit, O. Brandt, M. Ramsteiner, R. Uecker, P. Reiche, and K.H. Ploog, *J. Crystal Growth* **218**, 143 (2000).
28. P. Waltereit, O. Brandt, M. Ramsteiner, A. Trampert, H.T. Grahn, J. Menninger, M. Reiche, and K.H. Ploog, *J. Crystal Growth* **227**, 437 (2001).
29. P. Lefebvre, B. Gil, J. Allegre, H. Mathieu, N. Grandjean, M. Leroux, J. Massies, and P. Bigenwald, *MRS Internet J. Nitride Semic. Res.* **4S1**, G3.69 (1999).
30. T. Nishida and N. Kobayishi, *Phys. Stat Solidi* **176**, 45 (1999).
31. T. Detchprohm, K. Hiramatsu, H. Amano, and I. Akasaki, *Appl. Phys. Lett.* **61**, 2688 (1992).
32. R.J. Molnar, K.B. Nichols, P. Maki, E.R. Brown, and I. Melngailis, *Mater. Res. Soc. Symp. Proc.* **378**, 479 (1995).
33. N.R. Perkins, M.N. Horton, and T.F. Kuech, *Mater. Res. Soc. Symp. Proc.* **395**, 243 1996.
34. M. Ilegems, *J. Crystal Growth* **13**, 360 (1972)
35. S. Nakamura, *Jpn. J. Appl. Phys.* **30**, L1705 (1991).
36. D. Elwell, R. S. Feigelson, M. M. Simkins, W. A. Tiller, *J. Crystal Growth* **66**, 45 (1984).
37. We thank David C. Look at Wright State University for performing the Hall analysis.
38. P. Kung, A. Saxler, X. Zhang, D. Walker, R. Lavado, and M. Razeghi, *Appl. Phys. Lett.* **69**, 2116 (1996).

7th International Workshop on Advanced Infrared Technology and Applications AITA 2003

September 9–11, 2003
Scuola Normale Superiore Pisa, Italy
http://ronchi.iei.pi.cnr.it/AITA2003

The International Workshop on 'Advanced Infrared Technology and Applications' (AITA) is the seventh event of a series started in 1991. AITA constitutes a forum bringing together academic and industrial researchers to exchange knowledge, ideas and experiences in the field of infrared science and technology.

Chairman
L. Ronchi Abbozzo

Co-chairmen
G.M. Carlomagno, C. Corsi, E. Grinzato, I. Pippi, N.H. Rutt, O. Salvetti

Scientific Committee
D. Balageas, ONERA, Chatillon, France
J.M. Buchlin, VKI, Rhode-Saint-Genèse, Belgium
C.T. Elliott, Heriot-Watt University, Edinburgh, Scotland.
X. Maldague, Laval University, Quebec, Canada
E. Paganini, ENEL Produzione Spa, Pisa, Italy
A. Rogalski, Institute of Applied Physics, Warsaw, Poland
T. Sakagami, Osaka University, Japan
M. Strojnik, CIO, Leon Gto, Mexico
J.L. Tissot, ULIS, Veurey Voroize, France
V.P. Vavilov, Tomsk University, Russia
H. Wiggenhauser, BAM, Berlin, Germany
H. Zogg, ETH, Zurich, Switzerland

Topics
- Advanced technology and materials
- Smart sensors
- Thermofluid dynamics
- Far infrared
- Non-Destructive Evaluation
- Image processing and data analysis
- Advanced systems in cultural heritage, biomedicine, environment, aerospace, etc.
- Industrial applications

Abstracts Submission Guidelines
Submit a 300-500 words abstract electronically within March 15, 2003, indicating clearly title, name and affiliation of the Authors and the topic. Address, phone, fax number and E-mail of the corresponding Author must be also specified. Abstracts can be mailed to *AITA2003@isti.cnr.it* or submitted via Web (*http://ronchi.iei.pi.cnr.it/AITA2003*).

Deadlines
- March 15, 2003 Abstract submission
- April 30, 2003 Papers acceptance notification
- July 15, 2003 Final program delivery

Registration fees
- Euro 300, regular registration including: Social dinner, Coffee-breaks, Lunch, Abstracts and Proceedings
- Euro 150, student registration including: Coffee-breaks, Lunch and Abstracts

Publication
A book of abstracts of the accepted papers will be available at the workshop. Authors are also requested to deliver their contributions directly at the registration desk for proceedings publication. Furthermore, selected papers will be published in an international journal.

Language
English is the official language of the Workshop. All papers should be written and presented in English.

Technical Secretariat
Anna M. Meriggi
Fondazione Giorgio Ronchi
Via S. Felice a Ema, 20
50125 Firenze, Italy
Tel./Fax: +39 055 2320844
E-mail: *ronchi@infinito.it*

Organizing Secretariat
Ettore Ricciardi
CNR-ISTI, Via G. Moruzzi, 1
56124 Pisa, Italy
Tel.: +39 050 315 2907
Fax: +39 050 315 2810
E-mail: *ricciardi@iei.pi.cnr.it*

